Λ and Σ hyperons in nuclear matter

Asanosuke Jinno（神野朝之丞, KEK）

AJ, K. Murase, Y. Nara, and A. Ohnishi, Phys. Rev. C 108, 065803 (2023).
AJ, J. Haidenbauer, and U.-G. Meißner, Phys. Rev. C 112, 065209 (2025).

- **Motivation for studying hyperons in matter** (5slides)
- **Detailed analysis of Λ hypernuclei** (5 slides)
- **Λ and Σ single-particle potentials by YN force at N2LO** (12 slides)

APCTP, July 21-24, 2026.

Hyperons in matter ($T = 0$)

- **Hyperon: baryon including one or more strange quarks**
  E.g. Λ ~1116 MeV, $\Sigma^{0,\pm}$~1190 MeV (p, n ~ 940 MeV)
- **Naively, hyperons would appear as the neutron Fermi momentum increases.**
- **E.g. Free Fermi gas model with neutron and Λ**
  (Cf. A. Ambartsumyan & G. S. Saakyan (1960))

$$\mathcal{E}_{\mathrm{free}}(\rho_n, \rho_\Lambda) = g \sum_{i=n,\Lambda} \int_{|\boldsymbol{k}|<k_{Fi}} \frac{d^3\boldsymbol{k}}{(2\pi)^3} \sqrt{m_i^2 + \boldsymbol{k}_i^2},$$

$$P(\rho) = \rho^2 \frac{\partial}{\partial \rho} \left(\frac{\mathcal{E}_{\mathrm{free}}}{\rho} \right)$$

β equilibrium: $\mu_n = \mu_\Lambda, \quad \mu_i = \dfrac{\partial \mathcal{E}}{\partial \rho_i} = \sqrt{m_i^2 + k_{Fi}^2}$

Density: $\rho = \rho_n + \rho_\Lambda$

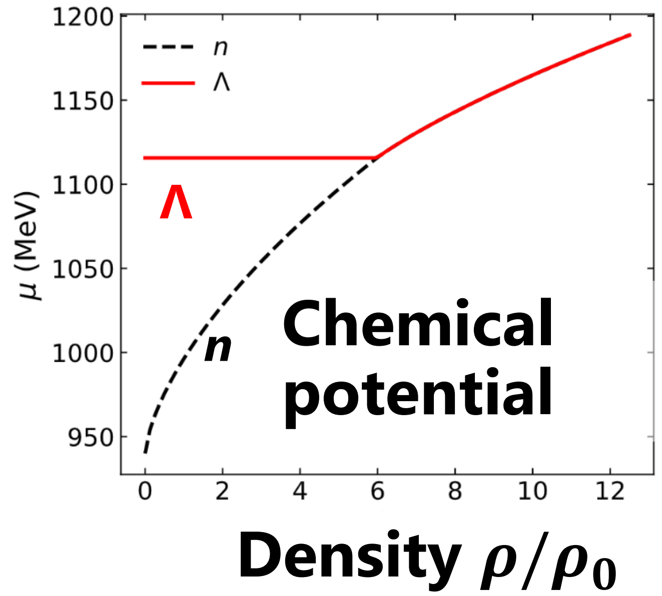

Softening

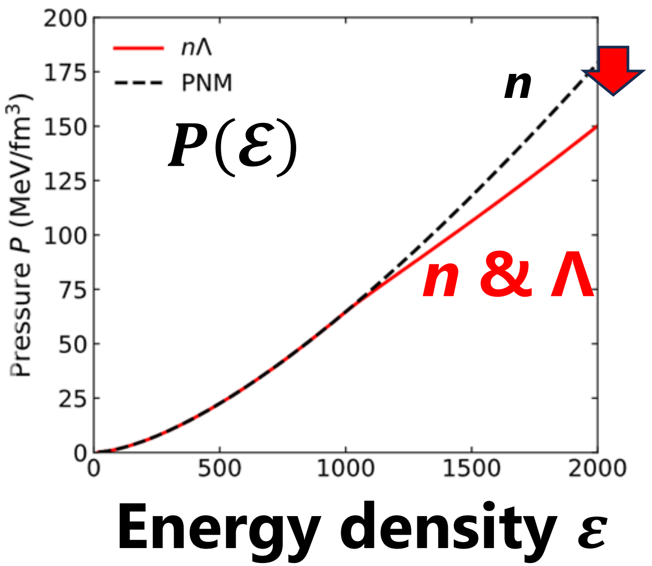

Hyperon puzzle

- **(1990-) Hyperon phenomenology predicts the appearance of hyperons in $2-4\ \rho_0$, <u>softening the EOS</u>.**

  e.g. N. K. Glendenning & S. A. Moszkowski PRL 67, 2514 (1991); R. Knorren, M. Prakash, & P. J. Ellis, PRC 52, 3470 (1995); S. Balberg & A. Gal, NPA 625, 435 (1997); S. Nishizaki, T. Takatsuka, and Y. Yamamoto, PTP 108 (2002) 703.

- **(2010-) First massive neutron star is reported, inconsistent with the hyperon phenomenology.**
  <u>Hyperon puzzle</u>

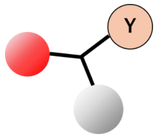

- **Example of solutions:**

  <u>Many-body forces (e.g. YNN)</u>

  e.g. D. Lonardoni, A. Lovato, S. Gandolfi, & Francesco Pederiva (2015).

  <u>Crossover between hadron and quark phases.</u>

  e.g. G. Baym, T. Hatsuda, T. Kojo, P. D. Powell, Y. Song, & T. Takatsuka (2018).

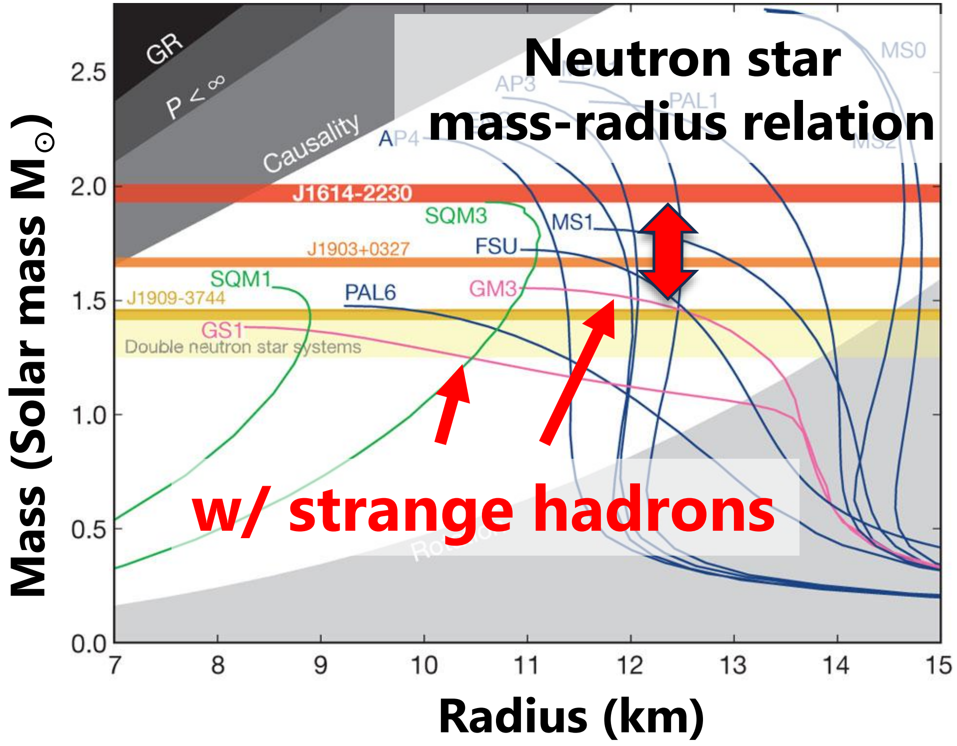

P. Demorest et al. Nature (2010).

Hyperon single-particle potential

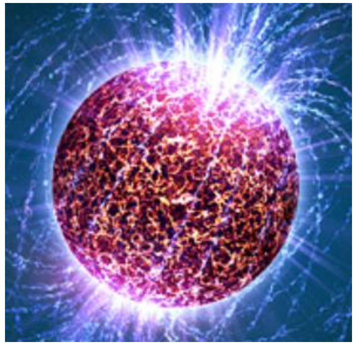

"I would contain no hyperon."

- **How about using our up-to-date knowledge on baryon interactions?**
- **<u>What quantity should be focused on?</u>**

Q. What is the condition that Λ hyperons appear in neutron stars?

A. (Neutron Fermi energy) > (Λ mass + <u>single-particle potential</u>)

≈ Mean value of the hyperon-medium nucleon interaction

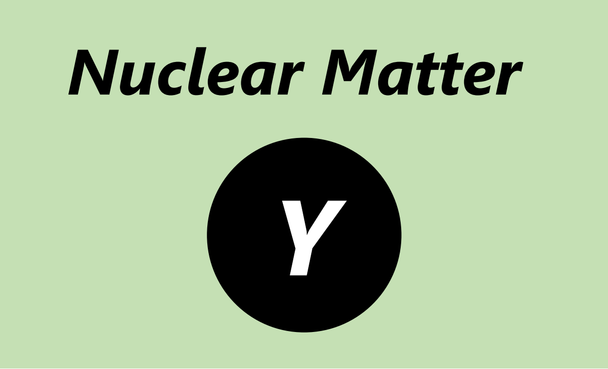

Current constraints on the single-particle potentials

✅ **Λ hypernuclear spectroscopy: $U_\Lambda(\rho_0) \approx -30$ MeV**

E.g. D. J. Millener, C. B. Dover, and A. Gal, (1988).

△ **Phenomenology based on e.g. Σ atoms: $U_\Sigma(\rho_0) = 30 \pm 20$ MeV**

A. Gal, E. V. Hungerford, & D. J. Millener (2016).

- **Λ directed flow created in heavy-ion collisions**

  Y. Nara, AJ, K. Murase, and A. Ohnishi, PRC 106 (2022) 044902.

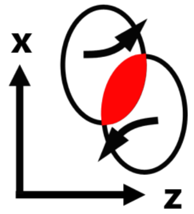

  Momentum dependence in the high momentum region should be determined to access to the density dependence.

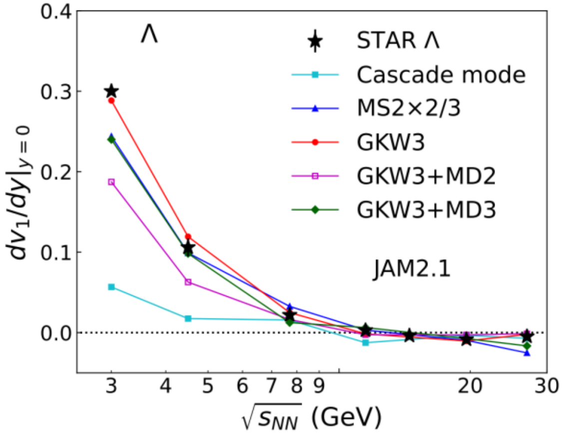

Lack of constraints at $\rho > \rho_0$.

Recent studies

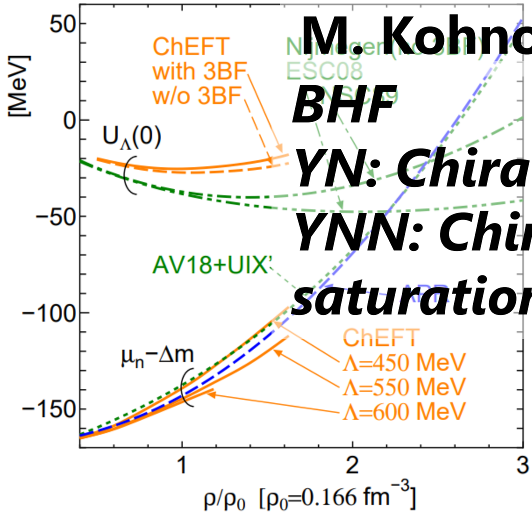

M. Kohno (2018)

BHF
YN: Chiral NLO13/19
YNN: Chiral decuplet saturation

D. Gerstung, N. Kaiser, W. Weise (2020)

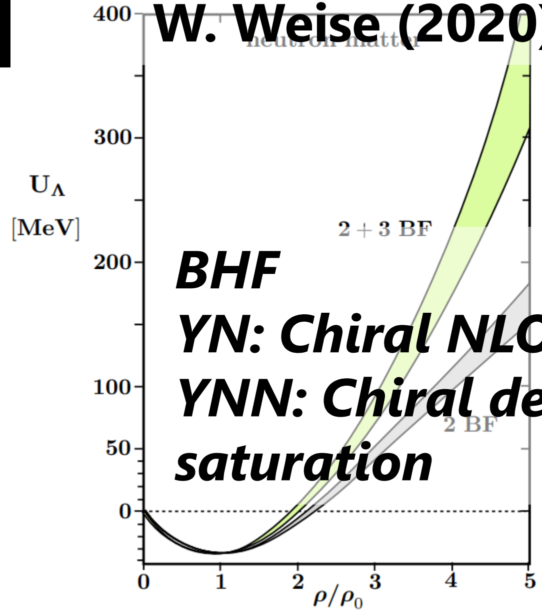

BHF
YN: Chiral NLO13/19
YNN: Chiral decuplet saturation

A. M. A. Looee, M. Shahrbaf, & M. R. Moshfegh (2026)

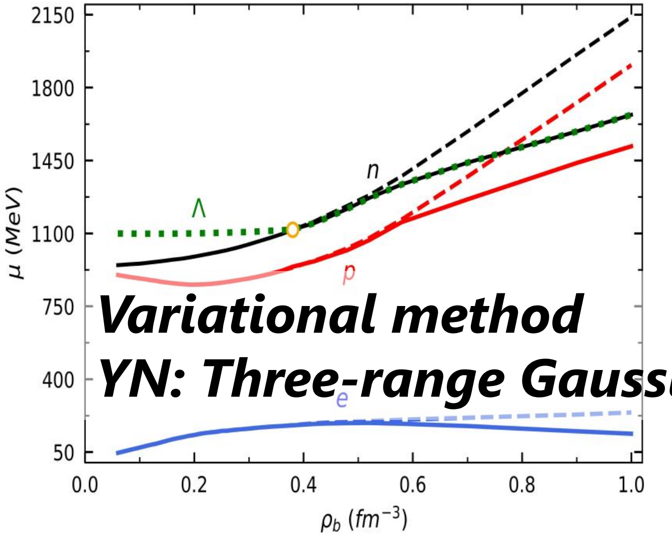

Variational method
YN: Three-range Gaussian

R. Zhenga, Z. Liua, L.-S. Genga, J. Hu, and S. Wang (2025)

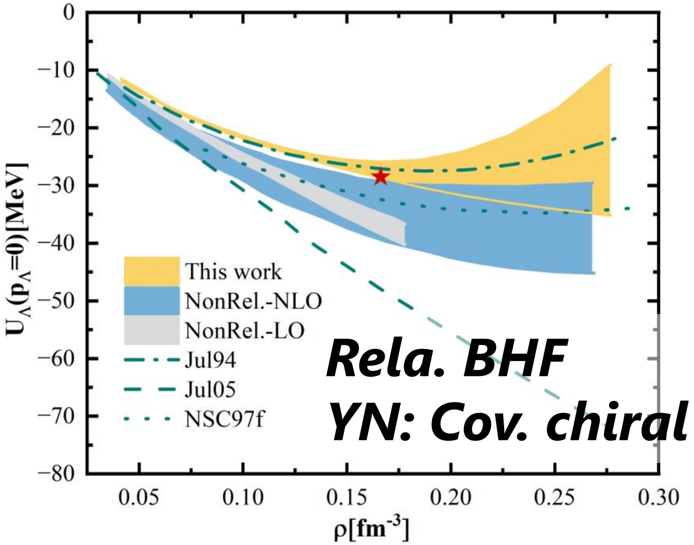

Rela. BHF
YN: Cov. chiral EFT at LO

D. L. Mihaylov, J. Haidenbauer, V. M. Sarti (2024)

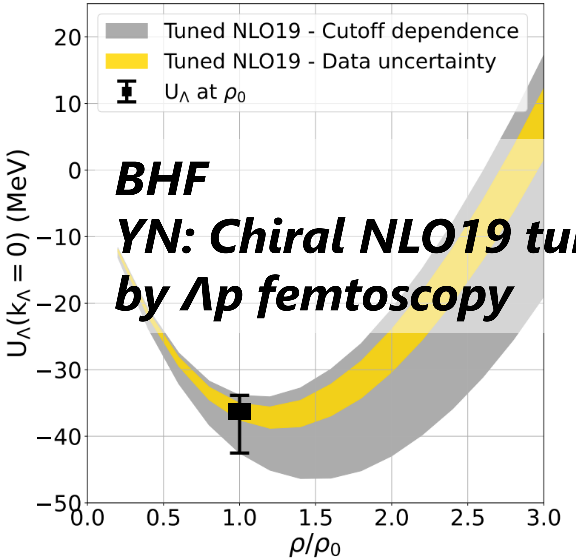

BHF
YN: Chiral NLO19 tuned by Λp femtoscopy

Application to neutron star matter:
I. Vidana et al. (2025)

Purpose of this study

Obtaining further constraints on Λ and Σ single-particle potentials by

① detailed analysis of Λ hypernuclei

② matter calculation based on up-to date chiral forces

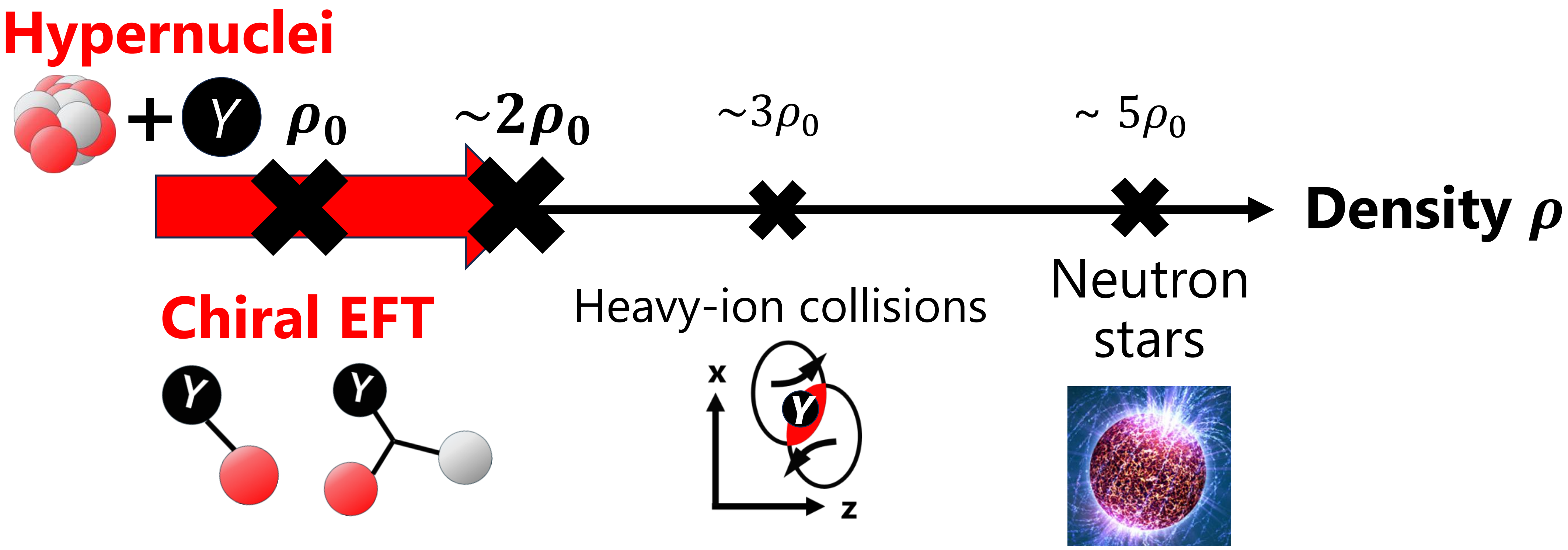

Detailed analysis ofΛ hypernuclei

(5 slides)

AJ, K. Murase, Y. Nara, and A. Ohnishi, Phys. Rev. C 108, 065803 (2023).

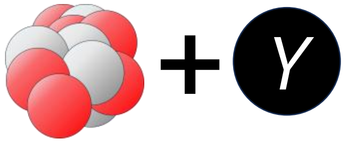

Λ binding energy

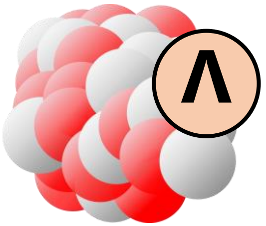

B_Λ : Λ binding (separation) energy

(1970-) Measured at CERN, KEK, BNL, JLab, and J-PARC, with mass number A=3–208.

Well-known information: $U_\Lambda(\rho_0) \approx -30$ MeV

Best fit study assuming Woods-Saxon type potential

A. Gal, E. V. Hungerford, & D. J. Millener, Rev. Mod. Phys. 88, 035004 (2016). (Original: D. J. Millener, C. B. Dover, and A. Gal (1988).)

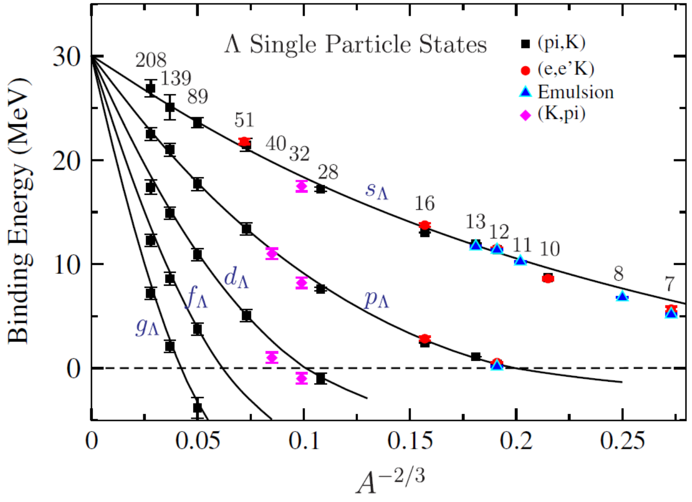

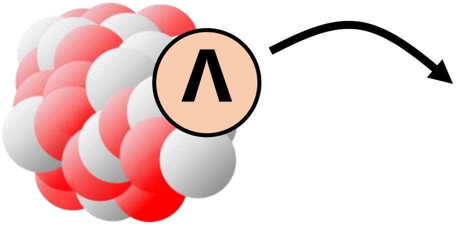

B_Λ : Λ binding (separation) energy

Many studies are done by best fitting.

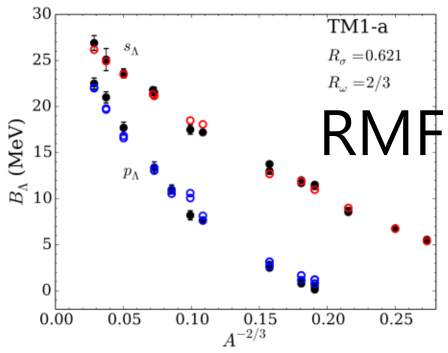

M. Fortin, S.S. Avancini, C. Providência, & I. Vidaña, PRC 95, 065803 (2017).

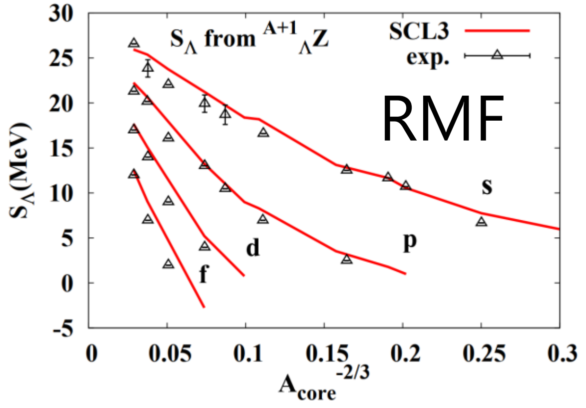

K. Tsubakihara, H. Maekawa, H. Matsumiya, and A. Ohnishi, PRC 81, 065206 (2010).

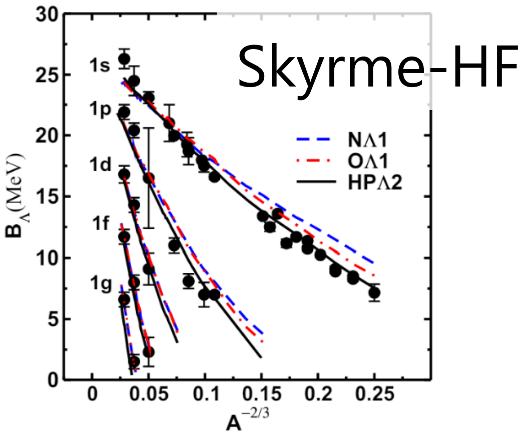

N. Guleria et al. NPA 886, 71 (2012).

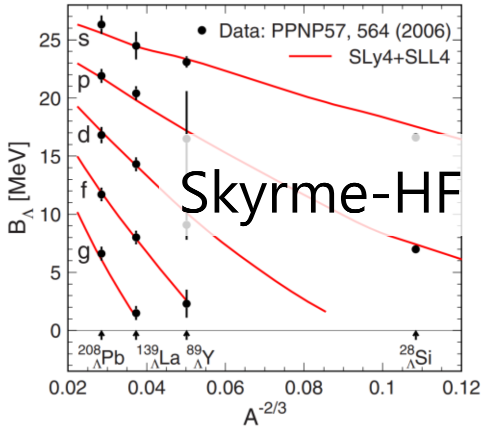

H.-J. Schulze and E. Hiyama, PRC 90, 047301 (2014)

The present constraints on $U_\Lambda(\rho)$ remain unclear.

Let’s systematically investigate the allowed range of $U_\Lambda(\rho)$!

Spherical Skyrme-Hartree-Fock

Cf. M. Rayet (1976) & (1981); D. E. Lanskoy and Y. Yamamoto (1997);
N. Guleria et al. (2012), H.-J. Schulze and E. Hiyama, PRC 90, 047301 (2014) etc.

density $\rho_N = \sum_{B=p,n} \sum_i |\psi_{B,i}|^2$

kinetic density $\tau_N = \sum_{B=p,n} \sum_i |\nabla\psi_{B,i}|^2$

Λ kinetic density $\tau_\Lambda = |\nabla\psi_\Lambda|^2$

Total energy of hypernuclei: $\mathcal{E}_{\mathrm{hyp}} = \mathcal{E}_N + \mathcal{E}_\Lambda - \mathcal{E}_{\mathrm{c.m.}}$

SLy4, E. Chabanat et al., NPA 635, 231 (1998).

$$\mathcal{E}_\Lambda = \int d^3r \, \underline{\frac{\hbar^2}{2m_\Lambda}\tau_\Lambda + a_2^\Lambda(\tau_\Lambda\rho_N + \tau_N\rho_\Lambda)}$$

$$\underline{+a_1^\Lambda\rho_\Lambda\rho_N + a_4^\Lambda\rho_\Lambda\rho_N^{4/3} + a_5^\Lambda\rho_\Lambda\rho_N^{5/3}} \; \underline{- a_3^\Lambda(\rho_\Lambda\nabla^2\rho_N)}$$

: Kinetic term

: Density dependent terms

: Surface term

By solving HF eq. $\delta\mathcal{E}_{\mathrm{hyp}}/\delta\psi_{B,i} = 0$ self-consistently,
Λ binding energy $B_\Lambda = \mathcal{E}_{\mathrm{core}} - \mathcal{E}_{\mathrm{hyp}}$ can be obtained

(Note) We here ignore deformation, pairing, spin-orbit interaction for Λ, and charge symmetry breaking of ΛN.

Analysis

Putting various $a_1^\Lambda, a_2^\Lambda, a_4^\Lambda, a_5^\Lambda$

Preparing 143,325 parameter sets

$\boldsymbol{a_3^\Lambda}$ is tuned to reproduce B_Λ of ${}^{13}_{\Lambda}\mathrm{C}$.

$$U_\Lambda = a_1^\Lambda \rho_N + a_2^\Lambda \tau_N - a_3^\Lambda \Delta\rho_N + a_4^\Lambda \rho_N^{4/3} + a_5^\Lambda \rho_N^{5/3}$$

$$\frac{\hbar^2}{2m_\Lambda^*} = \frac{\hbar^2}{2m_\Lambda} + a_2^\Lambda \rho_N$$

Calculating B_Λ^{cal} by solving Skyrme-Hartree-Fock eq.

Evaluating RMSD (root-mean-squared deviation) btw. B_Λ^{cal} and experiments:

$$\boldsymbol{\Delta B_\Lambda = \sqrt{\frac{1}{N}\sum\left(B_\Lambda^{\mathrm{exp}} - B_\Lambda^{\mathrm{cal}}\right)^2}}$$

${}^{208}_{\Lambda}\mathrm{Pb}$, ${}^{139}_{\Lambda}\mathrm{La}$, ${}^{89}_{\Lambda}\mathrm{Y}$, ${}^{56}_{\Lambda}\mathrm{Fe}$, ${}^{51}_{\Lambda}\mathrm{V}$, ${}^{40}_{\Lambda}\mathrm{Ca}$, ${}^{32}_{\Lambda}\mathrm{S}$, ${}^{28}_{\Lambda}\mathrm{Si}$, ${}^{16}_{\Lambda}\mathrm{O}$
s, *p*, *d*, *f*, *g* orbits ($N = 24$)
Including 0.5 MeV correction inferred via (π^+,K^+) reaction
T. Gogami et al., PRC 93, 034314(2016)

What type of Λ single-particle potential resulting in small RMSD ΔB_Λ?

(Result) Λ density dependence

AJ, K. Murase, Y. Nara, & A. Ohnishi, PRC 108, 065803 (2023).

U_Λ density dependence

RMSD $\Delta B_\Lambda < 0.75$ MeV

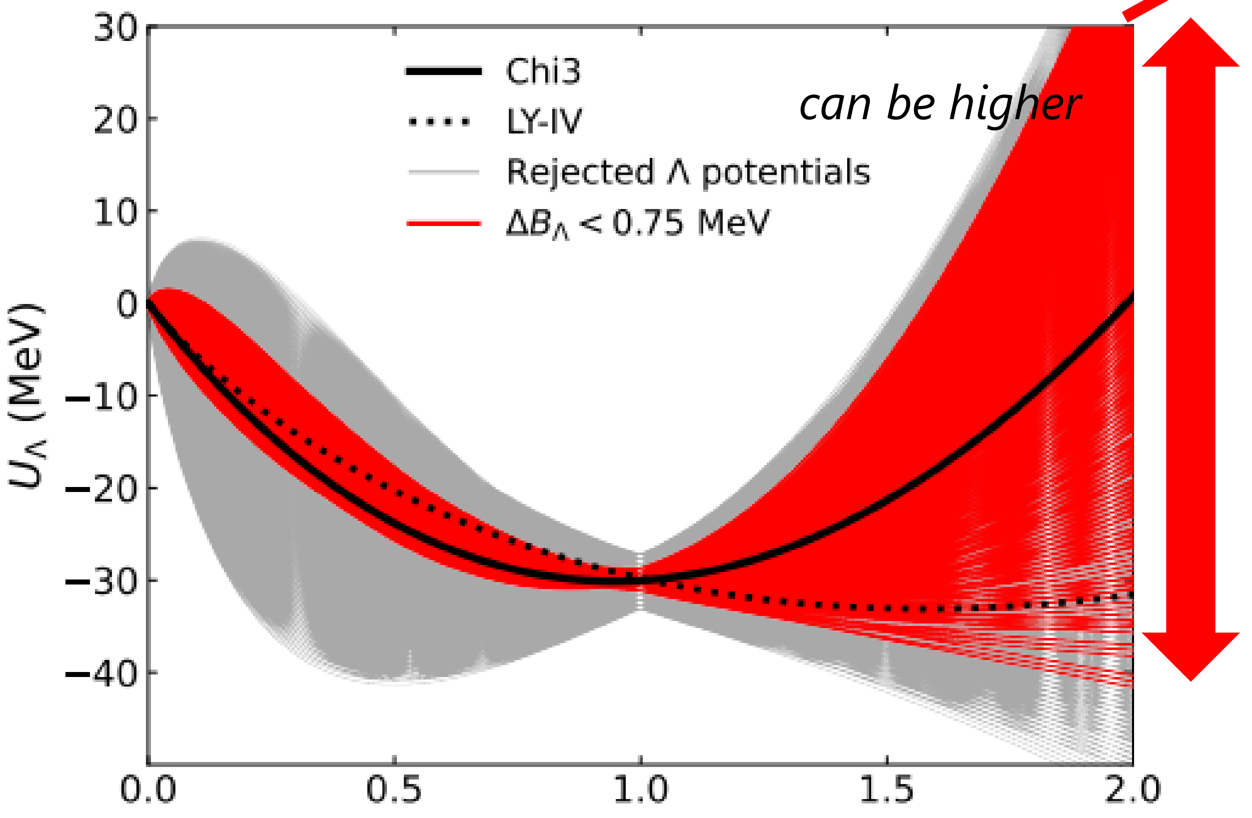

Density ρ/ρ_0

(Note) Decreasing the cut to 0.70 MeV does not change the range.

- $U_\Lambda(\rho_0) \approx -30$ MeV **(well-known)**
- $U_\Lambda(\rho_0 < \rho)$ **is constrained.**
- **Extrapolated region $U_\Lambda(\rho \gtrsim \rho_0)$ having lower limit.**

Λ and Σ single-particle potentials by YN force at N2LO

(12 slides)

AJ, J. Haidenbauer, and U.-G. Meißner, Phys. Rev. C 112, 065209 (2025).

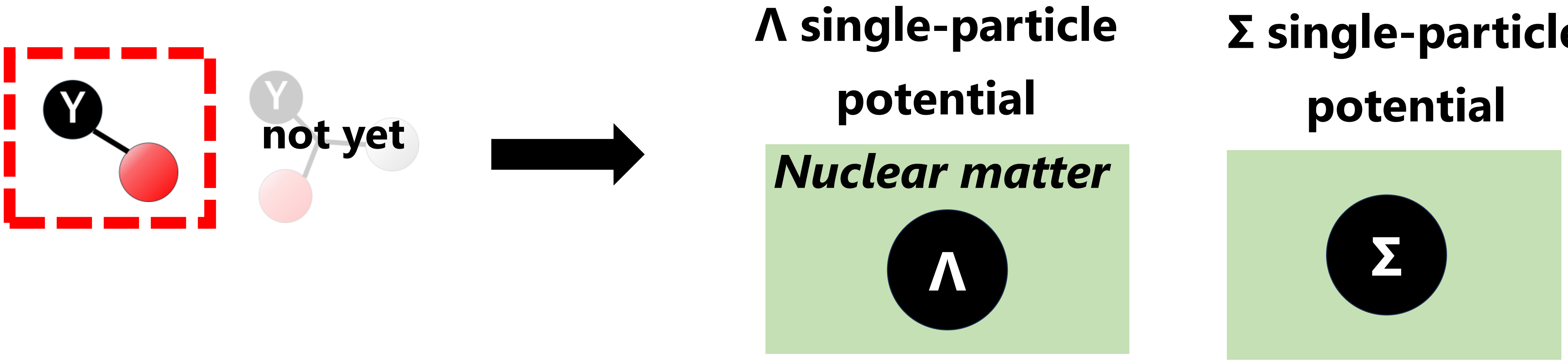

Hyperon-nucleon (YN) interaction studies

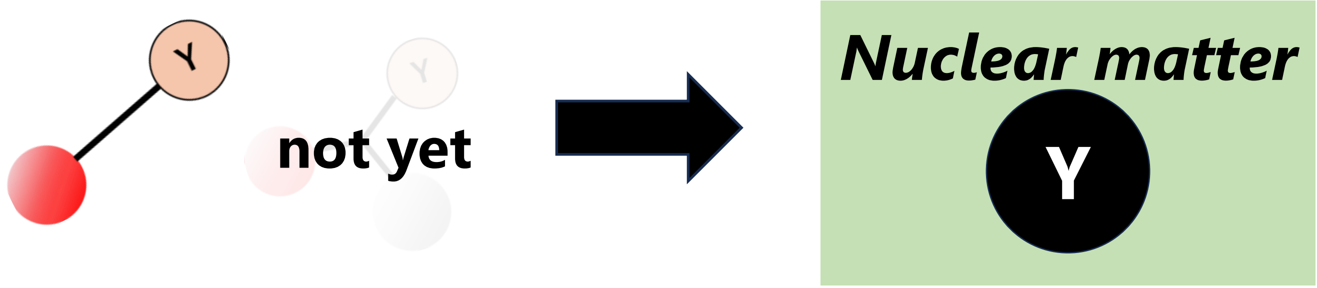

$\rho > \rho_0$?

- Boson exchange (e.g. Nijmegen, Jülich) and quark models (e.g. FSS, fss2):
  ✅ Physically intuitive construction △ Uncertainty estimate
- Lattice QCD（e.g. HAL QCD）
  ✅ Ab-initio calculation △ ΛN/ΣN and many-body forces
- <u>Chiral effective field theory</u>
  ✅ Systematic perturbative expansion, incorporating many-body forces
  △ Low-energy effective theory; valid for $\rho \lesssim 2\rho_0$ in normal nuclear matter

YN force studies by chiral EFT

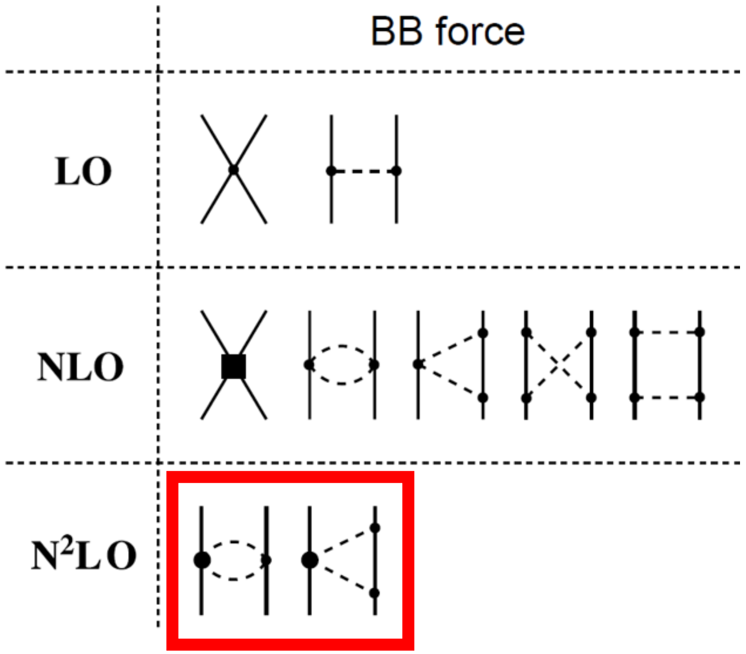

- LO in 2006: H. Polinder, J. Haidenbauer, & U.-G. Meißner.
- First version up to NLO (**NLO13**) in 2013
  J. Haidenbauer, S. Petschauer, N. Kaiser, U.-G. Meißner, A. Nogga, & W. Weise
- Alternative version up to NLO (**NLO19**) in 2019
  J. Haidenbauer, U.-G. Meißner, & A. Nogga
- **N2LO in 2023!**
  J. Haidenbauer, U.-G. Meißner, A. Nogga, & H. Le, Eur. Phys. J. A 59, 63 (2023).

N2LO YN force has several extensions from the NLO13 and NLO19 YN forces.

Review: J. Haidenbauer, Ulf-G. Meißner, & A. Nogga, arXiv:2508.05253

Extension in N2LO YN force

- J-PARC E40 data impose further constraints on 3S1 channel.

➢ Σ^+p: Nanamura et al., PTEP 2022, 093D01 (2022).
➢ Σ^-p: Miwa et al., Phys. Rev. C 104, 045204 (2021).

$\Sigma^+p - \Sigma^+p$

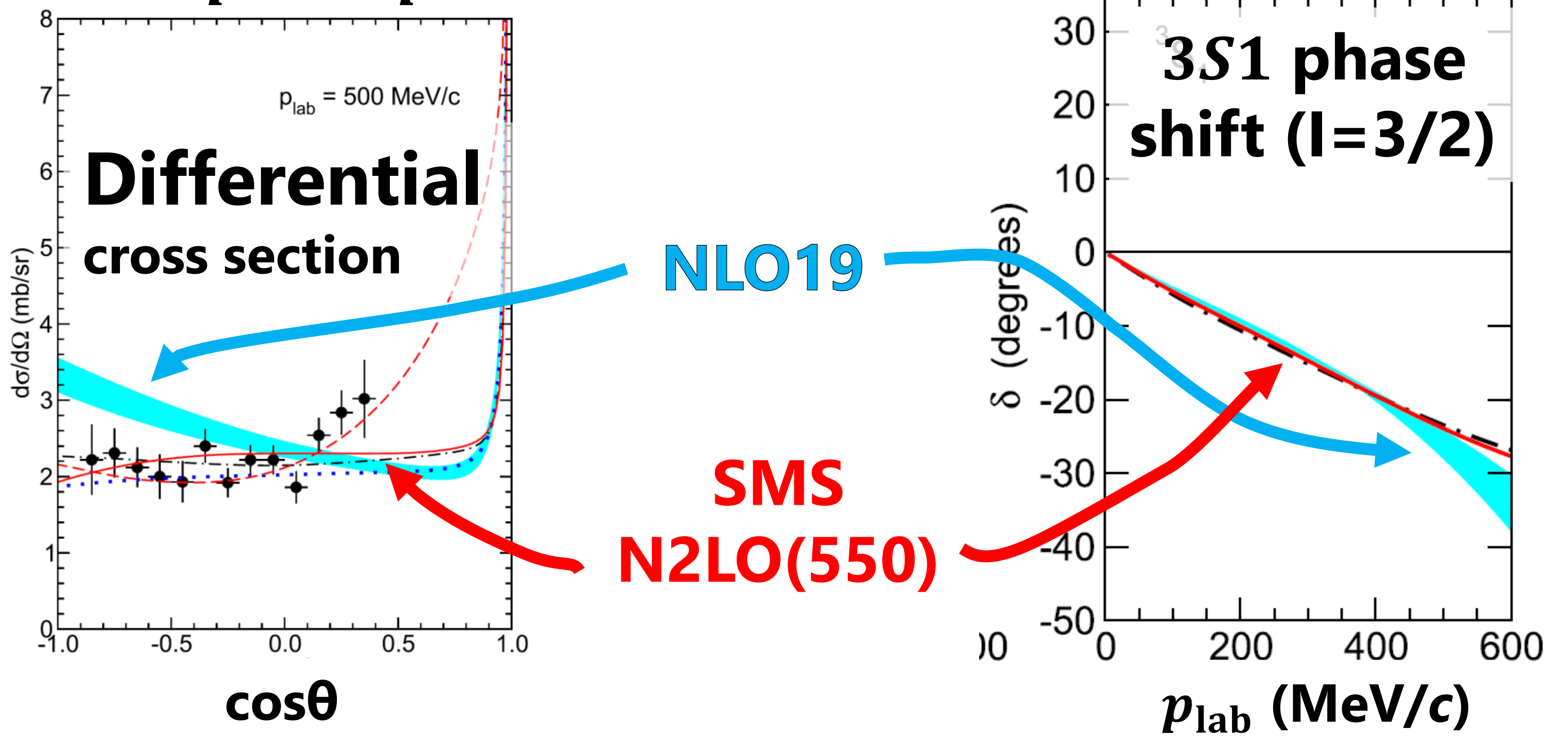

Black dash-dotted: SMS NLO(550)
Red solid: SMS N2LO(550)a
Red dashed: SMS N2LO(550)b. Readjusted P-wave LECs to produce an overall angular dependence
Cyan band: NLO19
Blue Dotted: NLO19(600) with a readjusted 3S1-3D1 LEC
Circle: J-PARC E40 data

How do hyperons in matter behave?

J. Haidenbauer, U.-G. Meißner, A. Nogga, H. Le, Eur. Phys. J. A 59, 63 (2023).

G matrix

K. A. Brueckner, C. A. Levinson, & H. M. Mahmoud (1954); Goldstone (1957)

Brueckner-Bethe-Goldstone equation

$$\boxed{G = v^{(2)} + v^{(2)}\frac{Q}{e}G,}$$

Pauli op.

$$Q\,|pq\rangle = \begin{cases} |pq\rangle & \text{for} \quad p, q > A \\ 0 & \text{otherwise} \end{cases}$$

$$e = \omega - H + i\epsilon \qquad H = m_1 + m_2 + \frac{(k_1)^2}{2m_1} + \frac{(k_2)^2}{2m_2} + \mathrm{Re}\,U_{B_1}(k_1) + \mathrm{Re}\,U_{B_2}(k_2)$$

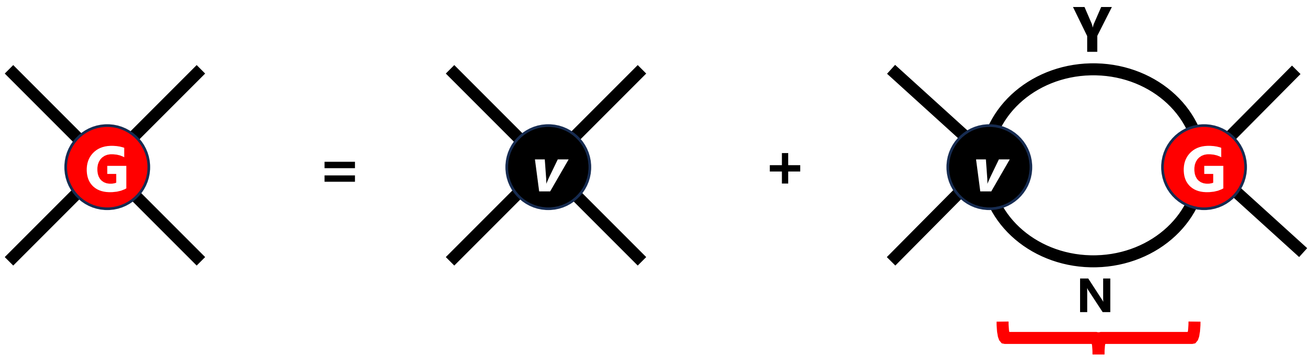

In-medium Lippman-Schwinger eq.

$\boldsymbol{Q = 0}$ **when** $\boldsymbol{k_N <}$ **Fermi momentum**

Single-particle potential

- **Single-particle potential can be chosen <u>arbitrary</u> and should be chosen to converge the hole-line expansion faster.**

- **Bethe-Brandow-Petschek theorem:**
  Many diagrams cancel out each other by taking the Hartree-Fock one:
  H. A. Bethe, B. H. Brandow, and A. G. Petschek, Phys. Rev. 129, 225 (1962).
  (Review) B. D. Day, Rev. Mod. Phys. 39, 719 (1967).

Self consistent

$$U_N = \sum_{m \leq A} \langle Nm | G(\omega = \epsilon_N + \epsilon_m) | Nm - mN \rangle,$$

$$U_Y = \sum_{m \leq A} \langle Ym | G(\omega = \epsilon_Y + \epsilon_m) | Ym \rangle,$$

$$G = v^{(2)} + v^{(2)} \frac{Q}{e(U)} G,$$

Setup

- NN: up-to-date chiral interaction SMS N4LO$^+$(450)

  P. Reinert, H. Krebs, and E. Epelbaum. Eur. Phys. J. A54(5), 86 (2018).

- YN: SMS up to N2LO

  NLO13 and NLO19 for comparison

- Non-relativistic Brueckner theory is utilized to evaluate the single-particle potentials.

  E.g. M. Kohno et al., NPA 674, 225 (2000), S. Petschauer et al., EPJA 52, 15 (2016).

$$\boxed{\begin{aligned} U_N &= \sum_{m\leq A} \langle Nm|G(\omega=\epsilon_N+\epsilon_m)|Nm-mN\rangle, \\ U_Y &= \sum_{m\leq A} \langle Ym|G(\omega=\epsilon_Y+\epsilon_m)|Ym\rangle, \end{aligned}}$$

$$\boxed{G = v^{(2)} + v^{(2)}\frac{Q}{\boldsymbol{e(U)}}G,}$$

Λ density dependence

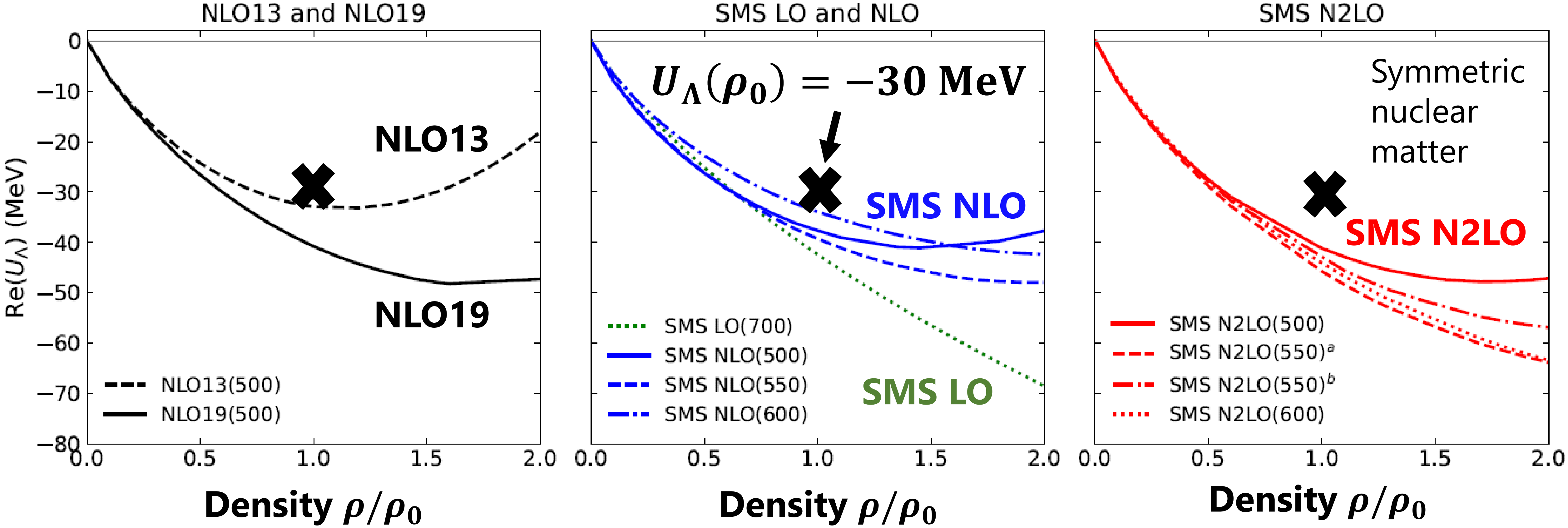

NLO19, SMS NLO and N2LO show similar trend, $U_\Lambda(\rho_0) = -45$ to -35 MeV

Cf. A recent phenomenological analysis:

$$U_\Lambda^{(\text{Two-body force})}(\rho_0) = -38.6 \pm 0.8 \text{ MeV}$$

E. Friedman and A. Gal, Nucl. Phys. A 1039, 122725 (2023).

YNN should make ≈ 10 MeV of repulsion at ρ_0.

Σ density dependence

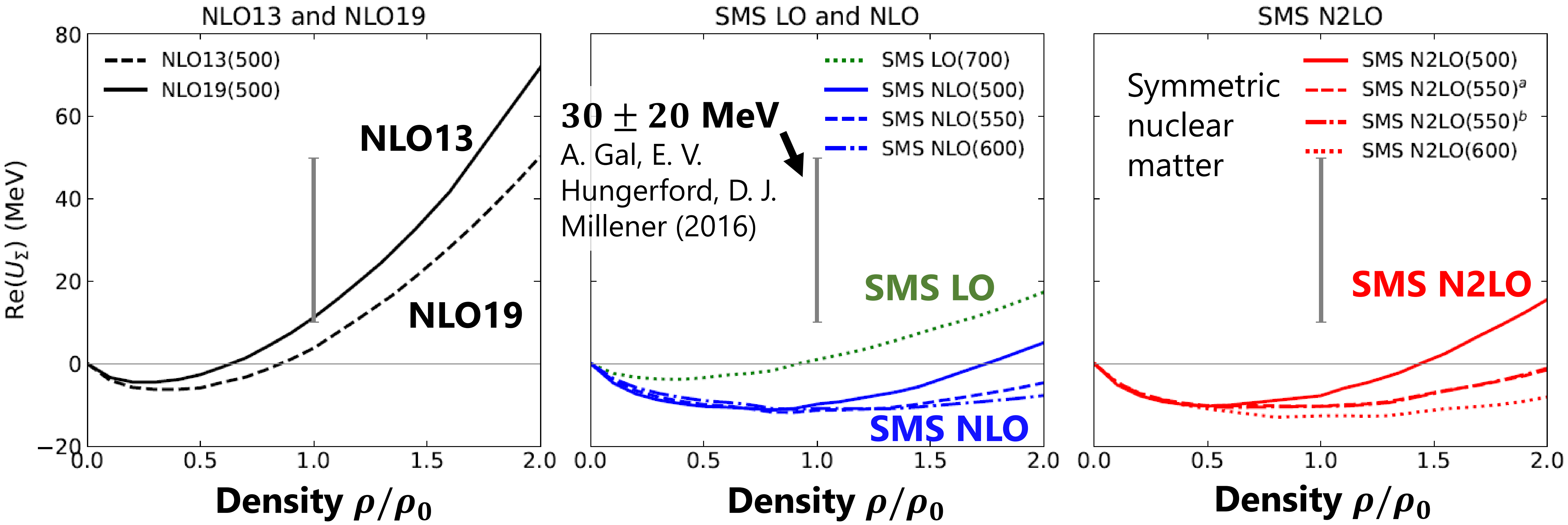

SMS NLO and N2LO yield more attractive $U_\Sigma(\rho_0) \approx -10$ MeV than NLO13 and NLO19, $U_\Sigma(\rho_0) \approx 10$ MeV.

(Note) Extraction of $U_\Sigma(\rho_0)$ from exp. data has many discussions: Cf. E. Oset et al., Phys. Rept. 188, 79 (1990); M. Kohno et al., PRC 74, 064613 (2006); T. Harada and Y. Hirabayashi, Phys. Rev. C, 107, 054611 (2023)

Σ partial-wave decomposition

	Isospin $I_0 = 1/2$			Isospin $I_0 = 3/2$		
	$^1S_0$	$^3S_1 + ^3D_1$	P	$^1S_0$	$^3S_1 + ^3D_1$	P
SMS LO(700)	7.1	−16.7	−1.9	−10.4	24.7	−1.5
SMS NLO(550)	8.0	−25.0	−0.3	−10.7	20.3	−3.4
SMS N^{2}LO(550)^a	7.5	−24.9	3.4	−11.0	20.0	−4.4
SMS N^{2}LO(550)^b	7.5	−24.8	3.6	−11.0	20.0	−5.0
NLO13(500)	6.2	−26.2	3.7	−11.1	32.5	−0.8
NLO19(500)	6.0	−19.5	3.8	−10.4	32.7	−0.8

Σ^+p elastic cross section

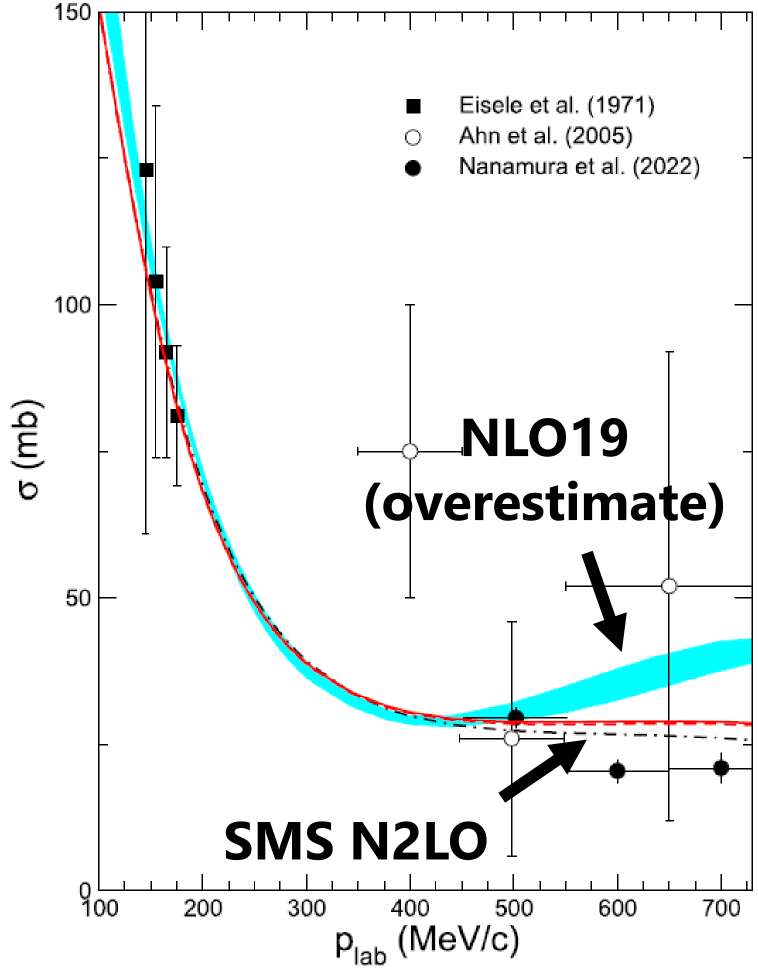

J-PARC E40 data constraint on the Σ^+p cross section leads to less repulsive isospin 3/2 channel (Σ^+p).

$\Sigma^+ p$ data: Nanamura et al., PTEP 2022, 093D01 (2022).

Σ^- in pure neutron matter

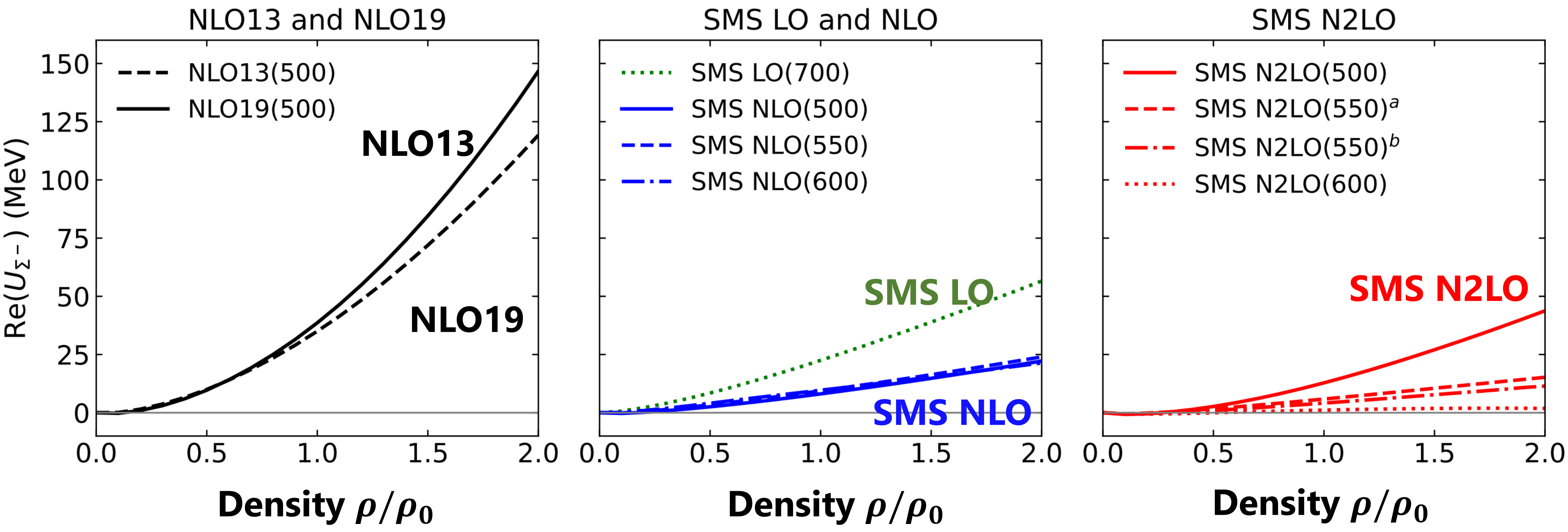

New SMS potentials yield less repulsive Σ^- potential in nuclear matter due to <u>less repulsive isospin 3/2 channel (Σ^-p)</u> by J-PARC E40 constraint.

Σ^- appears in neutron stars?

Uncertainty estimate (Truncation error)

- **Within chiral expansion, an observable X up to ith order is expressed as**

$$X^{(i)} = \underset{\mathcal{O}(Q^0)}{X^{\mathrm{LO}}} + \underset{\mathcal{O}(Q^2)}{\Delta X^{\mathrm{NLO}}} + \underset{\mathcal{O}(Q^3)}{\Delta X^{\mathrm{N2LO}}} + \cdots \Delta X^{i}$$

- **Error at ith order would be estimated as**

E. Epelbaum, H. Krebs, and U.-G. Meißner, PRL, 115, 122301 (2015).

$$\begin{aligned}
\delta X^{\mathrm{LO}} &= Q^2 \left|X^{\mathrm{LO}}\right|, \\
\delta X^{\mathrm{NLO}} &= \max\left(Q^3 \left|X^{\mathrm{LO}}\right|, Q \left|X^{\mathrm{NLO}} - X^{\mathrm{LO}}\right|\right), \\
\delta X^{\mathrm{N^2LO}} &= \max\left(Q^4 \left|X^{\mathrm{LO}}\right|, Q^2 \left|X^{\mathrm{NLO}} - X^{\mathrm{LO}}\right|,\right. \\
&\qquad \left. Q \left|X^{\mathrm{N^2LO}} - X^{\mathrm{NLO}}\right|\right),
\end{aligned}$$

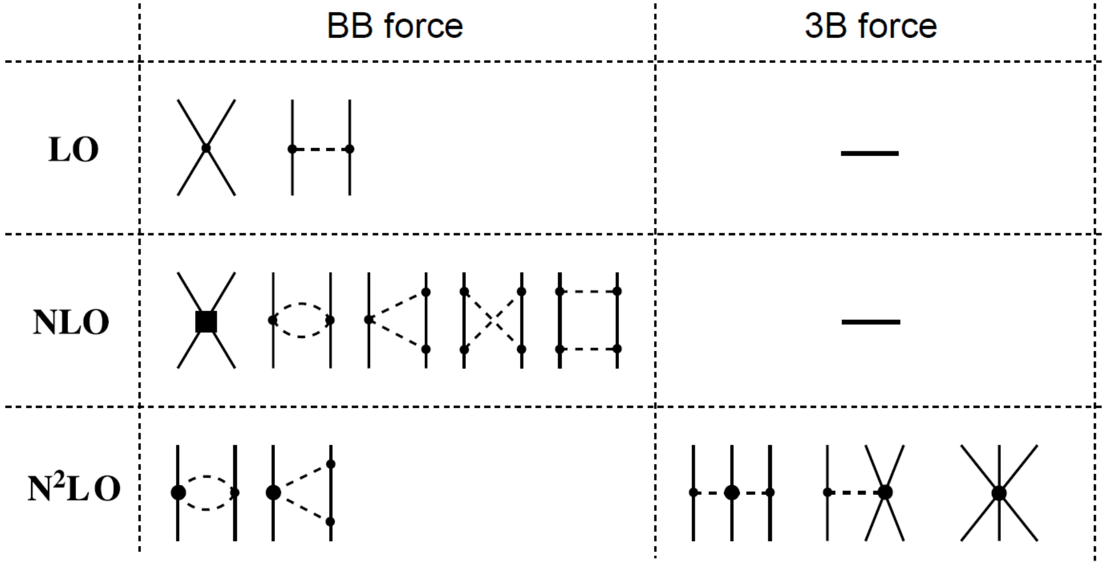

Adopted from E. Epelbaum's slide

- $Q = \max(p/\Lambda_b, M_\pi/\Lambda_b)$, p: **Fermi momentum.**

$\Lambda_b = 480$ MeV as inferred from a Bayesian method on nuclear matter

J. Hu, P. Wei, and Y. Zhang, Phys. Lett. B 798, 134982 (2019).

Uncertainty estimate

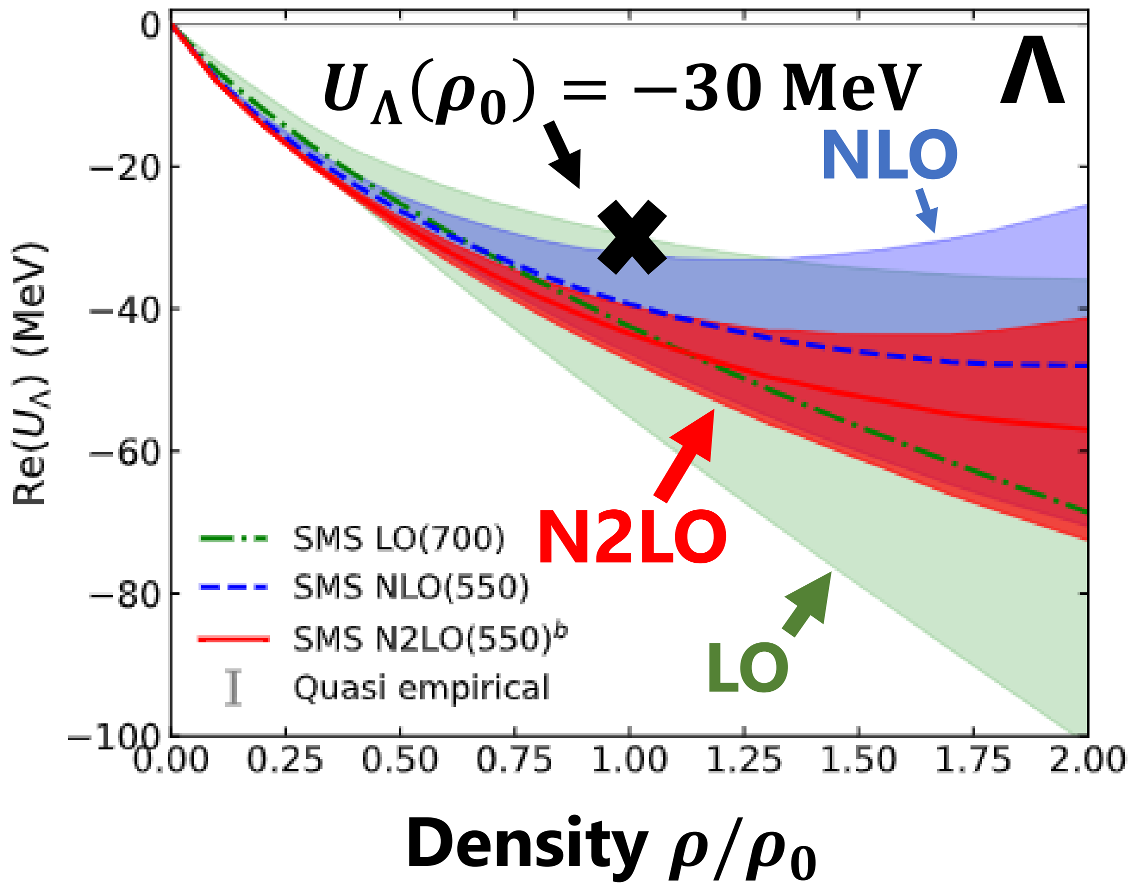

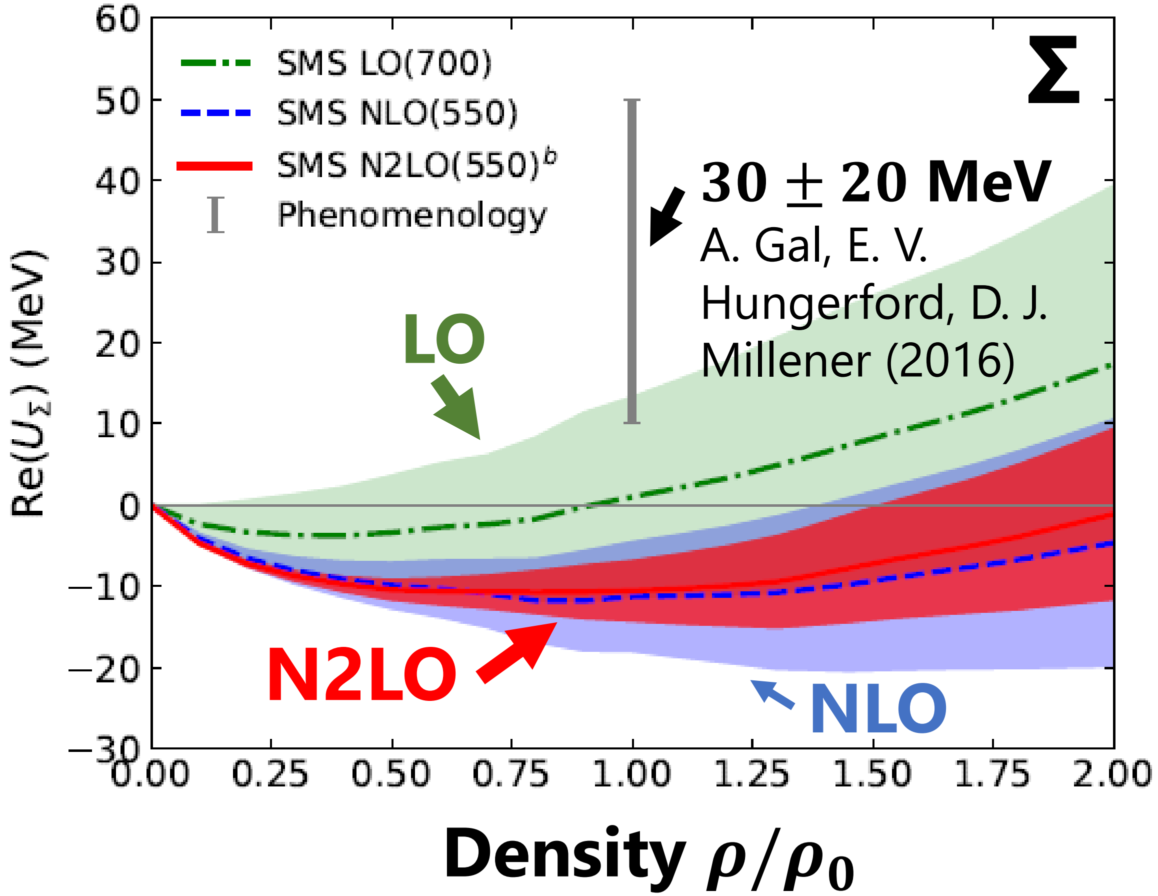

- **NLO error provides a glimpse on the size of YNN first appears at N2LO.**
- **YNN must create a repulsion at ρ_0, as one can see from the N2LO error.**

Summary (1/2)

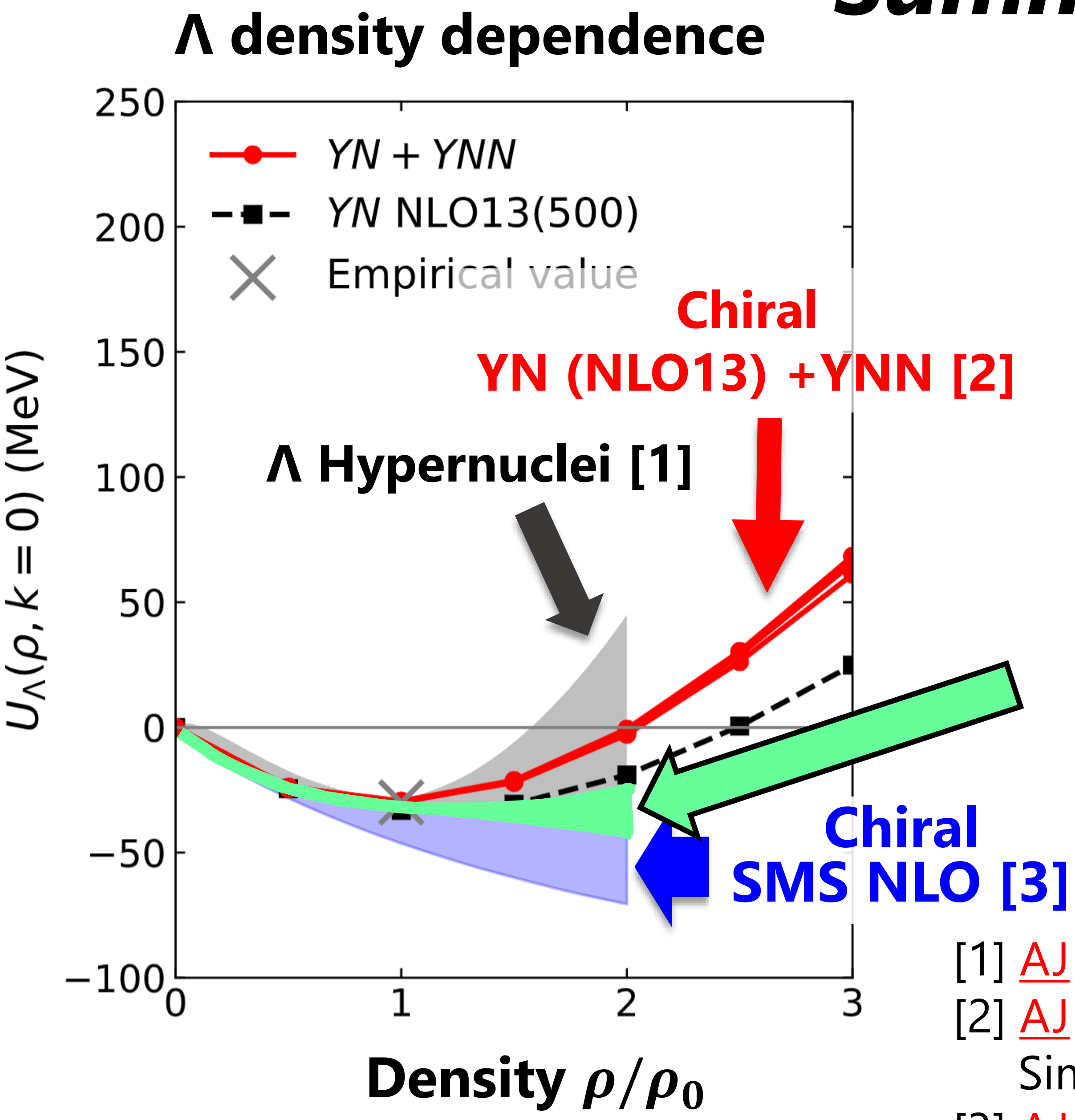

- **Combining the Λ hypernuclear constraint with the uncertainty band from chiral expansion.**
- **Overlapping region is more attractive than YN (NLO13)+YNN.**
- **<u>There may be hyperon puzzle within baryonic matter...?</u>**
  However, rigorous results can be obtained only after including YNN explicitly.

[1] AJ et al., PRC 108, 065803 (2023).
[2] AJ et al., PoS EXA-LEAP2024, 034 (2025).
Similar to D. Gerstung, N. Kaiser, and W. Weise (2020)
[3] AJ et al., PRC 112, 065209 (2025).

Summary (2/2)

- Σ single-particle potential U_Σ
- Chiral NLO YN+YNN: consistent with phenomenological band.
- Chiral SMS NLO error band: more attractive, reflecting J-PARC E40 data of ΣN scattering.

→ Is phenomenological error band OK?

<u>Can more Σ hypernuclei exist?</u>

Σ density dependence